11th International Workshop on Ship and Marine Hydrodynamics
Hamburg, Germany, September 22-25, 2019

Numerical analysis of unsteady hydrodynamic performance of pump-jet propulsor in oblique flow

Chengcheng Qiu[1,2], Guang Pan[1,2,*], Yao Shi[1,2]

[1]School of Marine Science and Technology, Northwestern Polytechnical University, Xi'an 710072, China
[2]Key Laboratory for Unmanned Vehicle, Northwestern Polytechnical University, Xi'an 710072, China

*Corresponding author, panguang@nwpu.edu.cn

ABSTRACT

In this study, the SST $k-\omega$ turbulence model and the sliding mesh technology based on RANS method has been adopted to simulate the exciting force and hydrodynamics of a pump-jet propulsor in different oblique flow angles (0°,10°,20°,30°) and different advance ratio (J=0.95,J=1.18,J=1.58).The full structured grid and full channel model has been adopted to improved computational accuracy. The time-domain data of pump-jet propulsor exciting force including bearing force and fluctuating pressure in different working conditions was monitored, and then converted to frequency domain data by fast Fourier transform (FFT). The various laws of bearing force in different advance ratio and different oblique flow angles has been presented. The results show that the exciting force will decrease with the oblique flow angle increases.And the closer which is to the rotor domain and the closer to the blades tip, the greater the variation of the pulsating pressure. At the same time, and the vertical forcea and transverse forces will change more obviously, which is the main cause of the exciting force. In addition, the pressure distribution of the rotor and stator blades in different oblique flow angles has been investigated.

1 INTRODUCTION

Pump-jet propeller is a special propeller, which has been widely used by military purpose for nuclear submarines and various types of torpedoes in the world. Compared with traditional propeller, the pump-jet propulsor has the wider application in underwater vehicles and submarines due to its high propulsion efficiency, low radiation noise and high critical speed. However, the pump-jet propulsor is working in oblique flow inevitably due to the influence of the ship's maneuvering state, irregular water flow, and navigation trim. The oblique flow has a great influence on the performance of the propulsor, which will cause the thrust and torque curves to shift relative to the open water state (Wang et al 2017). And the pump-jet propulsor blades are subjected to an unsteady load, causing the tail vibration and strong underwater noise. Therefore, it is important to study the various laws of the exciting force of the pump-jet propulsor in the oblique flow to improve the concealment and hydrodynamic performance. However, there are few studies about the pump-jet propulsor in the oblique flow due to the researches on pump-jet propulsor in oblique flow condition is complicated there.

At present, the research on pump-jet propulsor focuses on the hydrodynamic performance and cavitation in pure axial flow conditions by experiment and numerical simulation. Suryanarayana et al. (2010a, 2010b) presented the experiment of the pump-jet propulsor for an axisymmetric body in wind tunnel. The results verified the technique is useful and economical method for quick assessment of overall performance of the pump-jet propulsor. Lu et al (2016 and 2018) and Qin et al (2018) analyzed the different tip clearances effect on the hydrodynamic performance of pump-jet propulsor. The results found that the open water efficiency decrease as the size of the tip clearance increases, and the pressure distributions of the rotor and stator blades show that the pressure around the leading edge of rotor suction side is relatively low. Motallebi-Nejad et al (2017) analyzed the ducted propeller and pump-jet propulsion using periodic computational domain, the velocity and pressure distributions on pump-jet blades were shown and discussed. Oblique flow is a relatively simple non-uniform flow. At present, most of the research in the oblique flow of the propulsor is mainly focused on traditional propeller. Due to the complicated flow of the pump-jet propulsor, present

literature review that the various law of the excitation force and the hydrodynamic performance of the pump-jet propulsor in the oblique flow are few and far between. Dubbioso et al. (2013, 2014) analyzed the CNR-INSEAN E779A propeller in oblique flow with wide range of incidence angles (10°–50°) at two different loading conditions by overlapping grid approach. The main focus is on hydrodynamic loads (forces and moments) that act on a single blade, on the hub and on the complete propeller and peculiar characteristics of pressure distribution on the blade and downstream wake. Wang et al (2017) analyzed the DTMB4679 propeller exciting force in oblique flow based on RANS equations. The results shown that the oblique inflow angle has a greater influence on propeller unsteady bearing force than fluctuating pressure. Felli et al (2018) analyzed the underlying mechanisms of wake evolution and instability in oblique flow and the relation between the blade trailing wake and the instability of the tip and hub vortices by PIV experimental technique.

In this study, the SST $k-\omega$ turbulence model and sliding mesh technology based on RANS method were adopted to simulate the exciting force and hydrodynamic of the pump-jet propulsor in oblique inflow. The various laws of the six components of the bearing force and the change trend were calculated in different oblique inflow angles. According to the time-domain curve and the frequency domain curve, the various laws of bearing force had been analyzed in different advance ratio and different oblique flow angles. The pressure distribution in different oblique flow angles has been studied.

2 NUMERICAL SIMULAYION METHOD

2.1 Governing equation

The conditions of pump-jet propulsor flow in oblique inflow follow the law of conservation of mass, the law of conservation of momentum, and the law of conservation of energy. And water was the only single medium in our calculations, which was in-compressible fluid and whose heat exchange was ignored. The Reynolds time-average method is adopted to save the computational cost and calculation time, and the pulsation amount is introduced. The governing equations of the three-dimensional in-compressible and single phase fluid flows which are Reynolds Averaged Navier–Stokes (RANS) equations that can be written as the mass and momentum conservation in the following tensor form:

$$\frac{\partial \overline{u_i}}{\partial x_i} = 0 \tag{1}$$

$$\rho \frac{\partial \overline{u_i}}{\partial t} + \rho \overline{u_j} \frac{\partial \overline{u_i}}{\partial x_j} = \rho \overline{F_i} - \frac{\partial \overline{p}}{\partial x_j} + \frac{\partial}{\partial x_j}(\mu \frac{\partial \overline{u_i}}{\partial x_j} - \rho \overline{u_i' u_i'}) \tag{2}$$

Where ρ is the fluid density. x_i and x_j are the Cartesian coordinate components (i=1,2,3, j=1,2,3,). F is the body force on the micro element, which only considers gravity generally,the gravity was ignored in our calculations , so F equals zero. μ and P represent the dynamic viscosity and the pressure, respectively. μ_i and μ_j represents the absolute velocity component. $\rho \overline{u_i' u_j'}$ is the Reynold stress. $\overline{u_i}$ and $\overline{u_j}$ represents time-average value. $\overline{u_i' u_j'}$ represents pulsation value. The turbulence model is required to achieve the closure of Eq. (2).

2.2 Turbulence model

In the two-equation eddy viscosity turbulence model, the advantage of the $k-\varepsilon$ turbulence model is that it can simulate the turbulence flow, which is fully developed away from the boundary wall better. The advantage of the $k-\omega$ turbulence model is that it shows better applicability for boundary layer problems under different pressure gradients. The three different typical turbulence model SST $k-\omega$, Standard $k-\varepsilon$, Realizable $k-\varepsilon$ for the numerical simulation of the pump-jet propulsor were carried out by Qin et al. (2018). It indicated that the errors of Standard $k-\varepsilon$ and Realizable $k-\varepsilon$ turbulence model are a little bigger than

SST $k-\omega$ turbulence model. So the SST $k-\varepsilon$ turbulence model is chosen for the pump-jet propulsor numerical simulation. Its closed equations are shown in Eq. 3.

$$\left.\begin{aligned}\frac{\partial}{\partial t}(\rho k)+\frac{\partial}{\partial x_i}(\rho k u_i)&=\frac{\partial}{\partial x_j}(\Gamma_k\frac{\partial k}{\partial x_j})+G_k-Y_k+S_k\\ \frac{\partial}{\partial t}(\rho \omega)+\frac{\partial}{\partial x_i}(\rho \omega u_i)&=\frac{\partial}{\partial x_j}(\Gamma_\omega\frac{\partial k}{\partial x_j})+G_\omega-Y_\omega+S_\omega\end{aligned}\right\} \tag{3}$$

Where, G_k, G_ω are the turbulence kinetic energy production items, Γ_k, Γ_ω are the diffusion rate of the k and ω, Y_k, Y_ω are the turbulence dissipative items, S_k, S_ω are the source items.

3 COMPUTATION MODEL AND GRID

3.1 Model geometry

Pump-jet propulsor mainly has two types, which is front stator and rear stator. In this study, the rotor is in the front of the stator. And the pump-jet propulsor geometry model is shown in Fig.1. The pump-jet propulsor has 11 rotor blades, 9 stator blades. The simulation of pump-jet propulsor adopts full channel model to improve the accuracy of numerical simulation. Meanwhile, the pump-jet propulsor adopts the single stage rotor and stator system. The flow between of rotor and the inner wall of the duct needs to be considered, the tip clearance size between the rotor blade and duct is 1 mm.

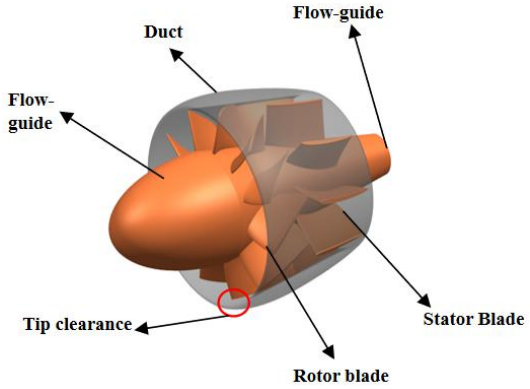

Fig.1.The pump-jet propeller model

3.2 Computational domain and Numerical grids

Fig.2. showed the computational domain and boundary conditions for pump-jet propulsor. Based on the shape of the pump-jet propulsor, the cylinder computational domain (13 D_{max} in length and 5 D_{max} in diameter) was selected. The inlet is located 4 D_{max} from the front face of pump-jet propulsor, and the outlet is situated 8 D_{max} from the end of pump-jet propulsor. D_{max} is the maximum diameter of the rotor blade. Fig.3. showed the rotating domain and stator domain. The computational domain is composed of three zones, which are the rotor domain, stator domain and external flow field domain. The rotor domain is a rotating domain, and stator domain and external flow field domain are stationary domains. In the study, the multi-reference frame (MRF) method is used for steady simulation to save computational costs and accelerate convergence, firstly. Then, the sliding grid method is applied for unsteady simulation, and the steady calculation results are used to initialize the flow field.

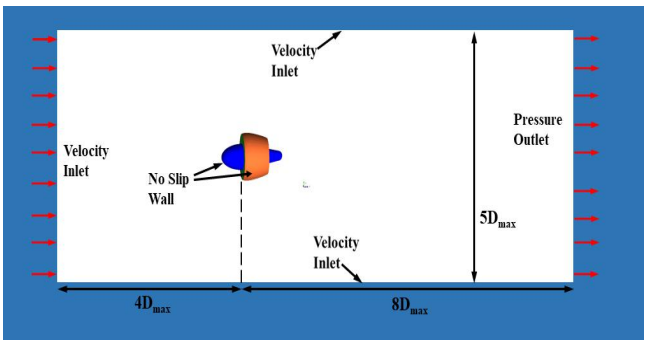

Fig.2.Computational domain and boundary conditions for pump-jet propulsor

The quality of the grid directly affects the accuracy and convergence of the calculation results. Fig. 4 showed the structured grids of stator and rotor blades surface. The grids around pump-jet propulsor adopted H-hybrid grids. The propulsor blade surface was surrounded by O-hexahedral girds, and the first layer mesh height is 0.05 mm. The flow fields in the rotor and stator domains change significantly, so the number of grids in these two fluid domains is relatively dense. The total number of grids is probably 7.2×10^6, including 3.99×10^6 rotor domain grids and 1.75×10^6 stator domain girds.

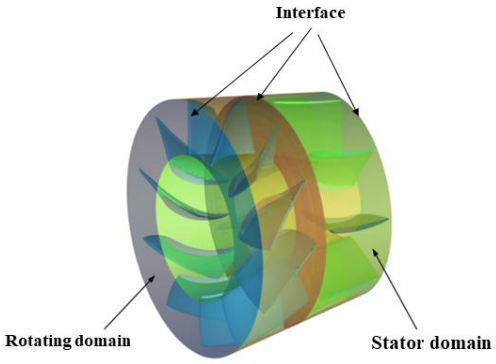

Fig. 3 Rotating domain and Stator domain

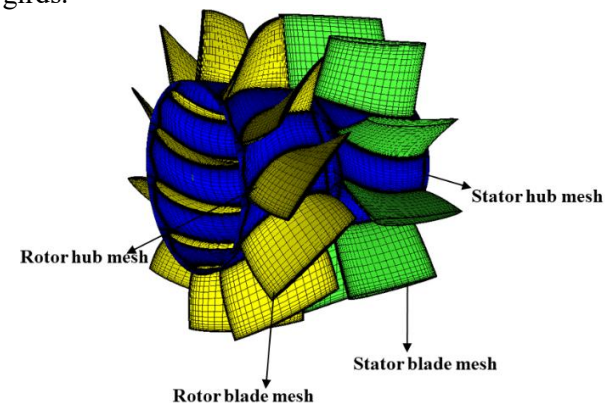

Fig. 4 Structured grids of stator and rotor

3.3 Boundary condition

In this study, the inlet boundary and the far field boundary are set as the velocity inlet boundary, the outlet boundary is set as the pressure outlet boundary. The operating pressure is set as 101325 Pa. Fig.5 showed that the diagram of oblique flow coming, numerical simulation of oblique flow conditions is achieved by varying the angle of attack in the horizontal plane x-z. U is the inflow velocity, β is the oblique flow angle. V_T is the tangential velocity component and V_Z is the axial velocity component in cylindrical coordinate system. The inflow velocity has been kept fixed to a value of U = 15.72 m/s, the different advance ratio J are achieved by changing the rotational speed of the propulsor. The calculation working conditions are shown in Table 1.

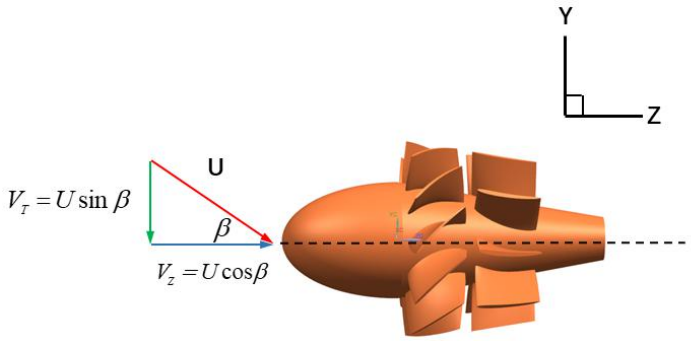

Fig.5 The oblique flow coming

Table 1 The calculation working conditions of pump-jet propulsor

	Working conditions group 1	Working conditions group 2	Working conditions group 3
Advance ratio J	1.58	1.18	0.95
Coming flow velocity (m/s)	15.72	15.72	15.72
Oblique flow angle (°)	0,10,20,30	0,10,20,30	0,10,20,30
Rotating speed (rpm)	2400	3200	4000

4 RESULTS AND DISCUSSION

4.1 Analysis of the variation laws of single-blade bearing force

In order to compare and analyze the various laws between the six pulsating components of the bearing force at different advance and different oblique inflow, all forces and moments are dimensionless:

$$\left.\begin{aligned} K_{Ti} &= \frac{T_i}{\rho n^2 D^4} \\ K_{Qi} &= \frac{Q_i}{\rho n^2 D^5} \end{aligned}\right\} \tag{4}$$

Where, i=x, y, z represent the Cartesian coordinate components, n is the rotation speed of pump-jet propulsor, D is the rotor diameter, T is the force and Q is the torque.

The exciting force of the pump propeller mainly includes bearing force and pulsating pressure. The bearing force is mainly composed of axial thrust, vertical force, transverse force and torque, vertical torque and lateral torque. Where the y direction is the vertical force,z direction is the axial thrust and the x direction is the transverse force.Fig 6 (a) and (b) show the change trend of the bearing force of the key rotor blade in different oblique flow angles when J=1.18 . From Fig 6 (a), it can be seen that the transverse force and vertical force decreases with the oblique flow angle increases. The transverse force and vertical force have obvious peaks and valleys in one cycle, and the peaks and valleys do not shift significantly in different oblique flow angles. The difference between the transverse force coefficient and the vertical force coefficient is smaller.At the same time, the transverse force coefficient and the vertical force coefficient of the rotor and stator have obvious phase difference in one cycle.

Fig.6 (b) shows the frequency domain variation curve of transverse force and axial force at different oblique flow angles. It can be seen that the transverse force has obvious fluctuations in the axial frequency (APF) and the blade frequency (BPF), indicating that the change of the oblique flow angle has a greater influence on the transverse force. At the axial frequency, the transverse force fluctuation amplitude decreases with the oblique angles increases. And vertical force also has similar trend.The axial force does not fluctuate at the axial frequency, and fluctuating slightly at the blade frequency, which indicating the oblique flow angle has little effect on the axial thrust.

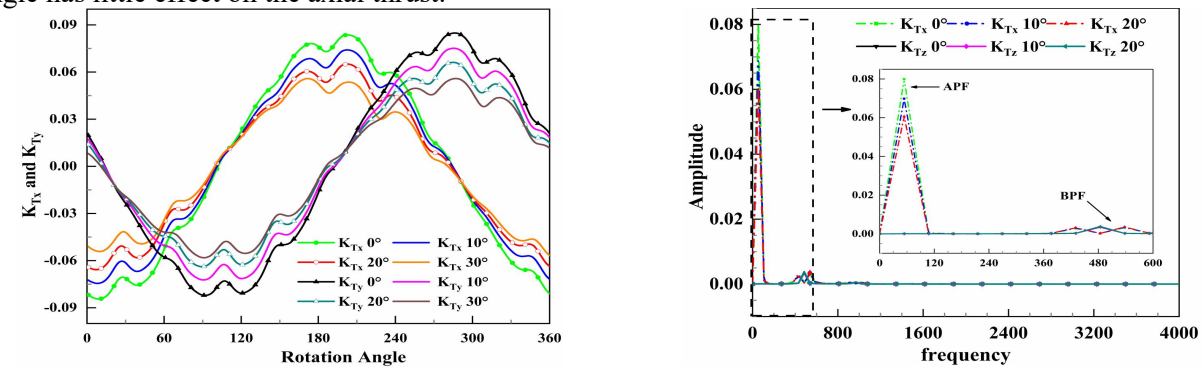

(a) The key rotor blade bearing force time-domain curve

(b) The key rotor blade bearing force frequency-domain curve

Fig.6 Time-domain and frequency-domain curve of different oblique flow angle

4.2 Analysis of pressure coefficient distribution`

In order to analyze the pressure various law of the rotor and stator blades, the pressure coefficient is defined as follows:

$$C_p = \frac{p_0 - p_r}{0.5\rho u^2} \tag{5}$$

Where the p_0 is the local pressure, p_r is the far field reference pressure, u is the velocity.

The Fig 7 (a) and (b) show that the distribution curves of the pressure coefficient of the rotor and stator blade at different oblique angles of r/R=0.4 and J=1.18, respectively. As can be seen from the figure 7 (a), the pressure coefficient increases with the oblique flow angle decreases at the leading edge of the rotor, and the fluctuation range is relatively consistent. The pressure coefficient decreases with the oblique flow angle increases, and the fluctuation range is relatively consistent. The difference of the rotor blade pressure is relatively large when the oblique flow angle is 0°, and it can provide greater pressure. It can be seen that the thrust output of the rotor blade reduces with the oblique flow angle increase. Compared with the rotor blade, the fluctuation range of the stator blade is relatively small with the oblique flow angle increases . It has the relatively obvious pressure gradient at the leading edge, then which transited to the edge smoothly. The pressure difference between the two sides of the blade decreases with the oblique flow angle increases, and the pump-jet propulsor total thrust decreases. The main reason for the difference is that the fluid pre-rotation of the propeller through the rotor, leading to the pressure fluctuation of the rotor blade obviously. Due to the action of the duct and the stator, the fluid of the pressure fluctuation in the stator blade is smaller, and the variation range of the stator pressure with the oblique flow angle is relatively stable.

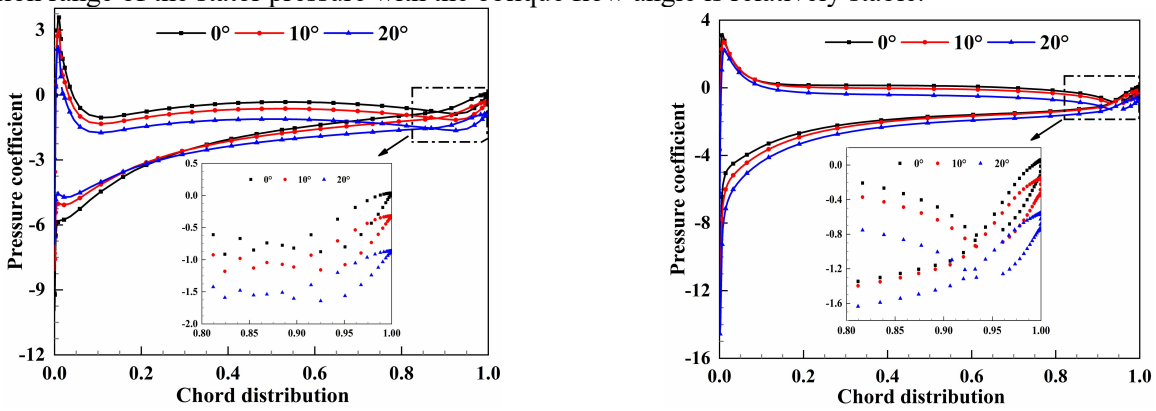

(a) r/R=0.4 the key rotor blade pressure coefficient distribution

(b) r/R=0.4 the key stator blade pressure coefficient distribution

Fig.7 Pressure coefficient distribution in different oblique flow angles(J=1.18)

5 CONCLUSION

In this study, the SST $k-\omega$ turbulence model and sliding mesh technology based on RANS method were adopted to numerically simulate the exciting force and hydrodynamic of the pump-jet propulsor in different oblique inflow angle (0°,10°,20°,30) and different advance ratio (J=0.95,J=1.18,J=1.58). The exciting force of pump-jet propulsor in different oblique flow angles is analyzed. The transverse force and vertical force decreases with the oblique flow angle increases. And the transverse force fluctuation amplitude decreases with the advance coefficient increases, where the axial force does not fluctuate at the axial frequency. And the pressure coefficient of the rotor and stator blades is analyzed. The pressure coefficient decreases with the increase of the oblique flow angle at the leading edge of the rotor and the fluctuation along the side. Compared with the fluctuation of the angle of the stator blade, the fluctuation of the rotor blade is more obvious.

ACKNOWLEDGEMENTS

This work is supported by the National Natural Science Foundation of China (Grant No. 51709229 and 61803306), the National Key Research and Development Project of China (Grant No.2016YFC0301300).

Our work is also supported by Natural Science Basic Research Plan in Shaanxi Province of China (Grant No. 2018JQ5092), and we are grateful for that.

REFERENCES

[1] Amini. H, Steen.S.2011.Experimental and Theoretical Analysis of Propeller Shaft Loads in Oblique Inflow. Journal of Ship Research. 55(4),1-21.

[2] Dubbioso G, Muscari R, Di Mascio A. 2013.Analysis of a marine propeller operating in oblique flow. Comput & Fluid.75:86–102.

[3] Dubbioso. G, R. Muscari, A. Di Mascio.2014. Analysis of a marine propeller operating in oblique flow. Part 2: Very high incidence angles. Computers & Fluids .92:56–81.

[4] Denghui Q, Guang P, Qiaogao H.2018. Numerical Investigation of Different Tip Clearances Effect on the Hydrodynamic Performance of Pump-jet Propulsor. Int. J. Comput. Methods. 15(5).

[5] Felli. M, Falchi. M, 2018.Propeller wake evolution mechanisms in oblique flow conditions.J. Fluid Mech.845:520-559.

[6] Lu, L., Pan, G., Sahoo, P.K., 2016. CFD prediction and simulation of a pumpjet propulsor. Int. J. Nav. Arch. Ocean Eng. 8 (1), 110-116.

[7] Lu L, Gao Y F, Li Q, Du L. 2018. Numerical investigations of tip clearance flow characteristics of a pumpjet propulsor. Int. J. Nav. Arch. Ocean Eng.10:307-317.

[8] Suryanarayana, C., Satyanarayana, B., Ramji, K., Saiju, A., 2010a. Experimental evaluation of pumpjet propulsor for an axisymmetric body in wind tunnel. Int. J. Nav. Arch. Ocean Eng. 2 (1), 24-33.

[9] Suryanarayana, C., Satyanarayana, B., Ramji, K., Saiju, A., 2010b. Performance evaluation of an underwater body and pumpjet by model testing in cavitation tunnel. Int. J. Nav. Arch. Ocean Eng. 2 (1), 57-67.

[10] Wang C, Sun S X, Sun S, Li L.2017. Numerical analysis of propeller exciting force in oblique flow. J Mar Sci Technol .22:602–619.